Challenges and Strategies for Drug Delivery Across the Blood–Brain Barrier: An Engineering Perspective

Mostafa Hany Tawfik*, Mostafa Mohamed*, Engy Mohamed*,
Omar Sherif§, Ziad Osama*, Moustafa Hani Ali*,
Mohamed Diaa Eldin§, Mohamed Abdelrazek*
*Systems & Biomedical Engineering Department
§Department of Electronics and Communications
Cairo University, Giza, Egypt
Emails: {Mostafa.hussien05, mostafa.ibrahim07, engy.elsarta05, omar.abdelkhaleq04,
Ziad.ebrahim04, moustafa.ali06, mohamed.elhosary06, Mohamed.Abdelrazek05}@eng-st.cu.edu.eg

***Abstract*—The blood–brain barrier (BBB) blocks most drugs from reaching the brain, making treatment of neurological diseases difficult. Focused ultrasound (FUS) with microbubbles offers a noninvasive way to temporarily open the BBB. After reviewing the literature on BBB structure, modulation techniques, and modeling approaches, we developed a four-part simulation pipeline: (1) converting CT scans to acoustic property maps using the Aubry method, (2) simulating acoustic wave propagation with a k-space pseudospectral solver, (3) modeling microbubble dynamics using the Marmottant equation, and (4) estimating thermal effects via the bioheat equation. At 1 MHz, we tested 21 source amplitudes from 30k to 500k Pa. Results showed that amplitudes between 70k and 210k Pa achieved safe and effective BBB opening, with peak negative pressure under 0.6 MPa, bubble radius under 10 μm, and temperature rise below 1°C.**

***Index Terms*—Blood-Brain Barrier, Focused Ultrasound, Microbubbles, Computational Modeling, Drug Delivery**

I. Introduction

Transporting therapeutic agents to the central nervous system (CNS) presents one of the most formidable challenges in pharmaceutical development, largely due to the presence of the Blood–Brain Barrier (BBB) [1], [2]. The BBB is a critical biological structure and a highly selective and dynamic interface, essential for maintaining CNS homeostasis by restricting the entry of blood-borne toxic compounds and pathogens. Unfortunately, this protective function also impedes the delivery of nearly all large-molecule therapeutics and over 98% of small-molecule drugs. Addressing this barrier is a major obstacle to advancements in treating key neurodegenerative diseases such as Alzheimer's, Parkinson's, and Epilepsy [3].

Overcoming this delivery bottleneck requires sophisticated strategies rooted in engineering and computational sciences. Research efforts are broadly divided into two areas: (1) developing novel material and biological strategies to circumvent or temporarily breach the barrier, often employing nanotechnology [4], and (2) utilizing computational and mathematical modeling to understand complex transport dynamics and predict drug efficacy in silico [5].

This review critically examines the current body of literature concerning the BBB, focusing on advanced engineering strategies for drug transport and the computational techniques used to model these processes. The main body synthesizes past studies across three key themes: the physiological nature of the barrier, modern material-based delivery platforms (nanocarriers and physical modulation), and the crucial role of mathematical and computational modeling, specifically highlighting the distinction between continuum (PDE-based) and agent-based methodologies [6]. Finally, this review identifies key gaps in current research to establish a clear framework for future studies.

A. Background: The Blood–Brain Barrier (BBB)

The BBB is anatomically defined by the neurovascular unit, primarily composed of brain capillary endothelial cells (ECs) tightly connected by specialized protein complexes, known as tight junctions (TJs) [3]. Unlike peripheral capillaries, brain ECs possess specialized TJs and often lack the fenestrations found in other endothelial layers. This barrier severely limits paracellular and transcellular flux. The BBB functions through multiple mechanisms: a physical barrier (TJs restricting paracellular movement), a transport barrier (efflux pumps), and a metabolic barrier (enzymes) [6].

The high stringency of the BBB restricts molecules based on their physicochemical properties, generally favoring small lipophilic molecules. Furthermore, active efflux transporters, notably P-glycoprotein (P-gp) and ATP-binding cassette (ABC) transporters, actively expel numerous drugs from the ECs back into the blood circulation, greatly reducing brain concentration. P-gp functions as a gatekeeper in the BBB [7]. The induction of P-glycoprotein overexpression is used in brain endothelial cells to model BBB efflux transport in vitro.

B. Challenges in CNS Drug Delivery

To deliver therapeutic agents across this highly restrictive interface, modern strategies exploit or temporarily modulate

the BBB's transport pathways.

C. Engineering Strategies for BBB Permeation

1) Nanocarrier-Based Targeted Delivery: Nanoparticle (NP) systems, which encapsulate drugs, have emerged as a primary strategy to improve CNS drug delivery [8]. Nanoparticles, designed as drug carrier systems, can facilitate central analgesic effects. These systems often employ the "Trojan Horse" strategy to hijack endogenous transport systems, relying on modifying NP surfaces with ligands to facilitate Receptor-Mediated Transcytosis (RMT) or Carrier-Mediated Transport (CMT).

Specific targets include:

- **Transferrin Receptor (TfR):** Targeting the TfR is a well-established method, enabling endocytosis-dependent antibody transcytosis across the BBB [9], [10]. This involves using TfR-targeted conjugates, antibodies, or specific aptamers attached to the carriers, which can enhance the uptake of the therapeutic agent. Nanoparticle brain uptake can be tuned by reducing the antibody's affinity for the TfR transcytosis target [11].
- **Low-Density Lipoprotein Receptor-Related Protein 1 (LRP1):** This receptor is exploited by vectors like Angiopep-2. Nanoparticles modified with Angiopep-2 have been shown to target glioma [12].
- **Amino Acid Transporters:** Prodrugs and nanocarriers can be modified to utilize carrier-mediated transporters like the L-type amino acid transporter 1 (LAT1) [12]. For instance, L-dopa conjugated liposomes loaded with WP-1066 showed in vitro uptake in LAT1-expressing cells. Phenylalanine-modified solid lipid nanoparticles loaded with Doxorubicin were found to deliver the drug into the brain at higher concentrations in rats compared to free drug. Conversely, the competing LAT1 substrate phenylalanine decreased the permeability coefficient of phenylalanine-modified solid lipid nanoparticles carrying efavirenz through co-cultured brain endothelial and astrocyte cells.

2) Physical Modulation: Focused Ultrasound (FUS): Physical methods can temporarily breach the barrier. One highly studied non-invasive technique involves Focused Ultrasound (FUS) combined with circulating microbubbles [13]. FUS can achieve localized delivery to the brain noninvasively.

D. Computational Modeling Paradigms

Computational models provide critical tools for studying the BBB, particularly for predicting drug partitioning and transport that would be difficult or impossible to test experimentally. Modeling approaches generally fall into continuum mechanics (PDEs) or discrete methods (Agent-Based Models).

1) Continuum Mechanics and PDE Models: Continuum models, often employing Partial Differential Equations (PDEs) or Computational Fluid Dynamics (CFD), are used to simulate processes like fluid flow and mass transfer [14]. These models can describe drug diffusion and elimination in brain tissue.

Mass Transfer and Microcirculation: Mathematical models focusing on molecular mass transfer across the BBB in brain capillaries have been developed. Solving the Navier-Stokes equation can calculate momentum and concentration profiles in each layer of the BBB and the brain parenchyma [9]. The dynamics of mass transfer involve convective flow in the capillary and diffusion in the layers surrounding the capillary, such as the endothelial cell layer and the astrocyte layer. Factors like capillary diameter and the influence of red blood cells (RBCs) can affect the concentration of nanoparticles [15]. Continuum models often assume homogeneity within subdomains. PDE models, sometimes coupled with Ordinary Differential Equations (ODEs) to integrate binding kinetics, are utilized to model the local drug distribution profiles within the brain. Such models include processes like diffusion and bulk flow in the extracellular fluid (ECF).

2) Agent-Based Modeling (ABM): ABM simulates systems by defining individual, autonomous components (agents) and their interactions. ABM is well-suited for modeling complex biological systems with heterogeneity and individual interactions [5].

Mechanistic Simulations: ABMs have been developed to model specific physiological processes at the BBB, such as cerebral glucose transport. ABM is used to model the transport of nanoparticles across the BBB. This approach simulates the behavior of particles under flow conditions, including Brownian motion and laminar flow. ABM can investigate parameters critical to RMT, such as ligand density and binding affinity (Ka) in in silico Transwell models of the BBB [12].

Disease Modeling (Multiple Sclerosis - MS): ABMs have been specifically applied to model autoimmune diseases like Multiple Sclerosis (MS), including Relapsing-Remitting MS (RRMS). Agents typically include self-reactive effector T cells (Teff) and regulatory T cells (Treg), along with virus and cytokine agents [16]. Cytokines released by activated Teff can modify BBB permeability. ABMs can simulate the effects of potential treatments by varying parameters like the probability of releasing cytokines that modify BBB permeability (`cytokine_probability`) and the BBB recovery times (`bbb_countdown`). For instance, a simulation showed that lowering the release of pro-inflammatory cytokines (by modifying `cytokine_probability` from 1 to 0.5 or 0.25) lowered unrecoverable damage. However, reducing the BBB recovery time (halving `bbb_countdown` from 50 to 25 time-steps) was found to be almost useless, either alone or coupled with lower cytokine probability, suggesting that prevention of permeability modification is better than restoration. Recent ABMs of MS also incorporate agents like Oligodendrocyte Precursor Cells (OPCs) and Perivascular Macrophages (PVMs), focusing on oligodendrocyte fitness and the Integrated Stress Response (ISR) as a therapeutic target for remyelination [15].

3) Predictive Machine Learning Approaches: Computational models are crucial for predicting BBB permeability in silico. Machine learning (ML) models are increasingly used for prediction [17], [18]. Recent efforts focus on developing ML

scoring approaches that outperform previous single molecular property methods like the Central Nervous System Multi-parameter Optimization (CNS MPO) approach. These ML models integrate novel and existing parameters derived from standardized databases. Predicting BBB penetration based on ML can use natural product databases [19].

II. Literature Review and Critical Analysis

The literature demonstrates significant advancement in both experimental techniques (like the development of improved in vitro BBB models using co-culture or microfluidics) and computational strategies.

A. Current Strengths in BBB Research

- **Nanocarrier Versatility:** Nanocarriers offer diverse strategies, utilizing various transport mechanisms like RMT and CMT, and can be designed to evade immune detection (e.g., PEGylation to reduce clearance by the reticuloendothelial system (RES)).
- **High Predictive Power of ML:** ML models, which rely on large, standardized datasets, provide improved predictive capabilities for binary BBB penetration and outperform traditional scoring systems when trained on enough data.
- **Mechanistic Detail in Modeling:** Continuum models, often incorporating the Navier-Stokes equation, provide quantitative, spatially explicit simulations of fluid flow and mass transfer dynamics. ABMs offer unparalleled flexibility to capture complex, individual-level interactions (e.g., ligand binding, cellular uptake, and specific immune cell dynamics in disease states like MS). For instance, ABMs helped demonstrate that preventing BBB permeability modification is superior to accelerating recovery (restoration) in MS treatments.

B. Identification of Research Gaps

1) Data Standardization Issues: The quality of predictive in silico models (ML/QSAR) is dependent on large, standardized databases. The absence of comprehensive, standardized experimental data can hinder the reliability of predictions.

2) Lack of Model Integration and Comparison: The literature uses both continuum (PDE/CFD) and discrete (ABM) approaches successfully. However, mathematical models typically focus on only a subset of crucial processes (e.g., focusing on BBB transport or intra-brain distribution, or binding kinetics). A noticeable gap exists in systematic studies that compare the results and suitability of these distinct modeling paradigms (PDE vs. ABM) for the same drug delivery challenge.

C. Rationale and Research Objectives

Recent advances in computational modeling have introduced hybrid approaches that combine agent-based modeling (ABM) with continuum mechanics and partial differential equations (PDEs) to simulate complex biological systems such as drug transport across the blood–brain barrier (BBB). While these methods offer high-resolution insights into cellular behavior and molecular diffusion, they often require extensive biological data and computational resources.

In this study, we adopt a physics-driven simulation strategy focused on the mechanical and thermal aspects of BBB opening via focused ultrasound (FUS). Rather than modeling drug transport directly, our rationale centers on predicting the physical conditions under which the BBB can be safely and effectively disrupted. By integrating CT-derived anatomical data with acoustic, bubble, and thermal simulations, we aim to identify safe operating windows for FUS exposure that maximize efficacy while minimizing risk.

III. Methodology and Simulation Framework

A. Pipeline Overview

To simulate the complex interaction between focused ultrasound (FUS) and the blood–brain barrier (BBB), we developed a modular simulation pipeline composed of four sequential stages. Each stage models a distinct physical phenomenon involved in BBB opening: acoustic wave propagation through the skull, microbubble dynamics under ultrasound exposure, and thermal effects due to acoustic energy absorption. The simulations were implemented entirely in Python using scientific computing libraries such as NumPy, SciPy, and Matplotlib. The anatomical basis for the simulations was derived from computed tomography (CT) imaging, which enabled spatially resolved modeling of skull and brain tissue properties.

The four simulation stages are:

1) Data Preprocessing
2) Acoustic Simulation
3) Microbubble Simulation
4) Thermal Simulation

B. Stage 1: Data Preprocessing and Property Mapping

1) The Aubry Method for CT Conversion: The first step involved converting CT scan data into spatial maps of acoustic properties. We used the Aubry method, which applies linear relationships between Hounsfield Units (HU) and acoustic parameters:

$$c(HU) = c_{\text{water}} + k_c \cdot HU \tag{1}$$

$$\rho(HU) = \rho_{\text{water}} + k_\rho \cdot HU \tag{2}$$

Where:

- $c_{\text{water}} = 1480$ m/s
- $\rho_{\text{water}} = 1000$ kg/m^3
- k_c and k_ρ are empirically derived constants

HU values were clamped to a range of $[-1000, 3000]$ to avoid outliers. The resulting maps of $c(x)$, $\rho(x)$, and $\alpha(x)$ (attenuation) were used as inputs for the acoustic simulation.

C. Stage 2: Acoustic Simulation

1) k-Space Pseudospectral Method: The propagation of ultrasound waves through the skull and brain was modeled using a k-space pseudospectral method, which efficiently computes spatial derivatives using Fast Fourier Transforms (FFTs).

2) Governing Wave Equations: The governing equation is the damped linear acoustic wave equation:

$$\frac{\partial^2 p}{\partial t^2} = c(x)^2 \nabla^2 p - 2\alpha(x)\frac{\partial p}{\partial t} + s(x,t) \tag{3}$$

Where:

- $p(x,t)$: acoustic pressure
- $c(x)$: spatially varying speed of sound
- $\alpha(x)$: attenuation coefficient (converted from dB/cm/MHz to Np/m)
- $s(x,t)$: source term representing the transducer

A single focused transducer was modeled by applying a phase delay across a linear source to focus energy at a predefined target point.

D. Stage 3: Microbubble Dynamics

1) The Marmottant Model: To simulate the behavior of microbubbles under ultrasound exposure, we implemented the Marmottant model, which accounts for the nonlinear dynamics of coated microbubbles.

2) Rayleigh–Plesset Shell Dynamics: The governing equation is a modified Rayleigh–Plesset equation:

$$\ddot{R} = \frac{1}{\rho R}\left(P_g - P_0 + P_{\text{ac}} - \frac{2\sigma(R)}{R} - \frac{4\mu\dot{R}}{R}\right) - \frac{3}{2}\frac{\dot{R}^2}{R} \tag{4}$$

Where:

- $R(t)$: bubble radius
- P_g: internal gas pressure
- $P_{\text{ac}}(t)$: acoustic pressure from the simulation
- $\sigma(R)$: surface tension, defined piecewise as:

$$\sigma(R) = \begin{cases} 0 & R < R_{\text{buck}} \\ \chi\left(\frac{R}{R_0} - 1\right) & R_{\text{buck}} \le R \le R_{\text{rupt}} \\ \sigma_{\text{water}} & R > R_{\text{rupt}} \end{cases} \tag{5}$$

This model captures the transition from buckled to elastic to ruptured states of the bubble shell. The maximum radial excursion of the bubble was recorded for each simulation to assess cavitation behavior.

E. Stage 4: Thermal Simulation

1) Bioheat Transfer Equation: Thermal effects due to ultrasound absorption were modeled using the bioheat transfer equation:

$$\rho c_p \frac{\partial T}{\partial t} = \nabla \cdot (k\nabla T) + Q_{\text{ac}} - \omega_b c_b (T - T_b) \tag{6}$$

Where:

- $T(x,t)$: temperature
- $Q_{\text{ac}} = 2\alpha I$: heat source from ultrasound absorption
- $I = \frac{p_{\text{rms}}^2}{\rho c}$: acoustic intensity from the pressure field
- ω_b: blood perfusion rate
- c_b: specific heat of blood
- T_b: baseline body temperature

The simulation was run over a 2D grid for a duration of 120 seconds to estimate the peak temperature rise at the focus.

F. Parameter Sweeping and Experimental Design

To explore the relationship between input amplitude and treatment outcomes, we performed a parameter sweep at a fixed frequency of 1 MHz, as supported by [20] on BBB opening. We tested 21 source amplitudes ranging from 30,000 Pa to 500,000 Pa. For each amplitude, we recorded: Peak Negative Pressure (PNP) at the focus, Maximum Bubble Excursion (μm), and Peak Temperature Rise (°C). This allowed us to identify safe and effective operating ranges based on mechanical and thermal safety thresholds.

IV. Results and Discussion

A. Simulation Parameter Definition

The following table summarizes the key physical and simulation parameters used across the four stages of the pipeline. These values were either extracted from literature, derived from CT imaging, or defined based on standard assumptions in the field of focused ultrasound-mediated BBB opening.

TABLE I
Simulation Parameters

Parameter	Value/Range	Unit	Source
Frequency (f_0)	1.0	MHz	Literature
Source Amplitude	30k – 500k	Pa	Sweep
Speed of Sound	1540	m/s	IT'IS DB
Density (brain)	1030	kg/m^3	IT'IS DB
Attenuation	0.7	dB/cm/MHz	He et al.
Bubble Radius (R_0)	2.0	μm	Definity
Shell Elasticity (χ)	0.5	N/m	Marmottant
Viscosity (μ)	0.001	Pa·s	Standard
Thermal Cond. (k)	0.5	W/m·K	IT'IS DB
Specific Heat (c_p)	3600	J/kg·K	IT'IS DB
Perfusion (ω_b)	0.01	s^{-1}	Bioheat
Blood Sp. Heat (c_b)	4180	J/kg·K	Standard
Baseline Temp (T_b)	37	°C	Physio.

B. Analysis of Parameter Sweep Outputs

To evaluate the effect of input amplitude on treatment outcomes, we performed a parameter sweep at a fixed frequency of 1 MHz. For each of the 21 tested amplitudes, we recorded the outputs shown in Table II.

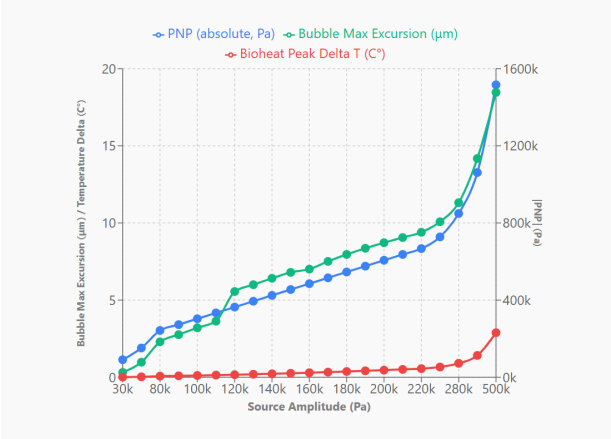

Fig. 1. Graphical Summary for simulation results

TABLE II
PARAMETER SWEEP RESULTS

Run	Source (Pa)	—PNP— (Pa)	Bub Max (μm)	ΔT (°C)
1	30,000	90,961	0.317	0.0104
2	50,000	151,602	0.974	0.0289
3	80,000	242,563	2.297	0.0739
4	90,000	272,884	2.762	0.0936
5	100,000	303,204	3.207	0.1155
6	110,000	333,525	3.635	0.1398
7	120,000	363,845	5.554	0.1664
8	130,000	394,165	5.999	0.1952
9	140,000	424,486	6.415	0.2264
10	150,000	454,806	6.798	0.2599
11	160,000	485,127	7.009	0.2957
12	170,000	515,447	7.508	0.3339
13	180,000	545,767	7.960	0.3743
14	190,000	576,088	8.360	0.4170
15	200,000	606,408	8.719	0.4621
16	210,000	636,729	9.053	0.5095
17	220,000	667,049	9.396	0.5591
18	240,000	727,690	10.075	0.6654
19	280,000	848,972	11.312	0.9057
20	350,000	1,061,215	14.177	1.4151
21	500,000	1,516,021	18.458	2.8880

C. Physical Response Interpretation

The results reveal a strong, nonlinear relationship between the source amplitude and all three output metrics. As expected, increasing the amplitude leads to higher peak negative pressures, greater bubble excursions, and more pronounced temperature rises. However, the rate of increase is not uniform across the range.

1) Acoustic Pressure and Non-linearity: The peak negative pressure (PNP) increases approximately linearly with source amplitude up to $\approx$ 300,000 Pa, after which the slope becomes steeper. This suggests that skull-induced nonlinearities and constructive interference at the focus may amplify pressure beyond a certain threshold. Importantly, the mechanical index (MI), derived from PNP and frequency, also increases with amplitude, indicating a higher risk of inertial cavitation at higher drive levels.

2) Bubble Cavitation Regimes: The bubble excursion follows a similar trend. Below 100,000 Pa, the oscillations remain small and stable. Between 100,000 and 210,000 Pa, the bubble enters a regime of stable cavitation, characterized by controlled oscillations without collapse. Beyond 240,000 Pa, the excursion exceeds 10 μm, indicating a transition toward inertial cavitation, which is associated with potential tissue damage and uncontrolled BBB disruption.

3) Thermal Load and Bioheat Effects: Temperature rise remains negligible ($<$0.1°C) for amplitudes below 150,000 Pa. However, as the amplitude increases beyond 300,000 Pa, the thermal load becomes significant, with ΔT exceeding 1°C at 350,000 Pa and reaching nearly 3°C at 500,000 Pa. While these values are still below thermal ablation thresholds, they may contribute to unwanted biological effects, especially with repeated exposures.

D. Identification of the Safe Operating Window

Based on the literature and safety guidelines, we defined the following thresholds:

- PNP $\leq$ 0.6 MPa
- Bubble excursion $\leq$ 10 μm
- ΔT $\leq$ 1°C

The amplitude range of **70,000 to 210,000 Pa** satisfies all three criteria. This range provides sufficient acoustic pressure to open the BBB while maintaining thermal and mechanical safety. It also aligns with reported values in preclinical studies, reinforcing the validity of the simulation framework.

V. LIMITATIONS AND FUTURE DIRECTIONS

A. Geometric Constraints: 2D vs. 3D Modeling

All simulations were conducted on a single 2D axial slice extracted from a CT scan. This approach significantly reduces computational complexity and allows for rapid prototyping and parameter exploration. However, it does not fully capture the three-dimensional anatomical variability of the skull and brain, nor the volumetric nature of ultrasound propagation. Future work should extend the framework to 3D volumetric simulations, which would enable more accurate modeling of beam focusing, skull curvature effects, and off-axis energy deposition.

B. Microbubble Population Heterogeneity

The microbubble simulation assumed a single, monodisperse bubble with a fixed initial radius of 2.0 μm. In reality, contrast agents such as Definity or Sonovue contain a distribution of bubble sizes, each responding differently to acoustic pressure. Incorporating a polydisperse bubble population model would provide a more realistic estimate of cavitation behavior and improve predictions of BBB opening efficacy and safety.

C. Integration of Pharmacokinetic (PK) Models

This study focused exclusively on the mechanical and thermal aspects of BBB opening. However, the ultimate goal of FUS-mediated BBB disruption is to enhance drug delivery. Future extensions of this work should include models of molecular transport across the BBB, such as diffusion, convection, and clearance mechanisms. Coupling the current framework with pharmacokinetic and pharmacodynamic (PK/PD) models would enable a more complete prediction of therapeutic outcomes.

D. Requirements for Experimental Validation

While the simulation results align with published safety thresholds and expected trends, the framework has not yet been validated against experimental or clinical data. Future work should involve comparison with in vitro or in vivo measurements of pressure, cavitation, and temperature rise to calibrate and validate the model parameters.

VI. Conclusion

This study presents a complete and reproducible simulation framework for modeling focused ultrasound-mediated blood–brain barrier (BBB) opening. By integrating anatomical data from CT imaging with physics-based models of acoustic propagation, microbubble dynamics, and thermal effects, we were able to simulate and evaluate the safety and efficacy of ultrasound exposure across a wide range of input amplitudes. The simulation pipeline was divided into four stages: (1) data preprocessing using the Aubry method to convert CT Hounsfield Units into acoustic property maps, (2) acoustic simulation using a k-space pseudospectral solver, (3) microbubble modeling via the Marmottant equation, and (4) thermal estimation using the bioheat equation. A parameter sweep at 1 MHz across 21 amplitudes (30k–500k Pa) revealed that the range of 70k–210k Pa consistently produced safe and effective outcomes. Within this range, the peak negative pressure remained below 0.6 MPa, bubble excursions stayed under 10 μm, and temperature rise did not exceed 1°C — all within accepted safety thresholds for BBB opening. These findings not only validate the simulation approach but also provide a practical reference for selecting ultrasound parameters in future experimental and clinical studies. The modular structure of the framework allows for easy extension to 3D modeling, real-time feedback integration, and drug transport simulation. As such, this work lays a strong foundation for future in silico planning and optimization of FUS-based neurotherapies.

References

[1] H. Wang, Z. Zhang, J. Guan, W. Lu, and C. Zhan, "Unraveling GLUT-mediated transcytosis pathway of glycosylated nanodisks," *Asian J. Pharm. Sci.*, vol. 16, no. 1, pp. 120–128, Jan. 2021, doi: 10.1016/j.ajps.2020.07.001.

[2] W. M. Pardridge, "Drug Transport across the Blood–Brain Barrier," *J. Cereb. Blood Flow Metab.*, vol. 32, no. 11, pp. 1959–1972, Nov. 2012, doi: 10.1038/jcbfm.2012.126.

[3] Q. He *et al.*, "Towards Improvements for Penetrating the Blood–Brain Barrier—Recent Progress from a Material and Pharmaceutical Perspective," *Cells*, vol. 7, no. 4, p. 24, Apr. 2018, doi: 10.3390/cells7040024.

[4] E. Kirit, C. Gokce, B. Altun, and A. Yilmazer, "Nanotherapeutic Strategies for Overcoming the Blood–Brain Barrier: Applications in Disease Modeling and Drug Delivery," *ACS Omega*, vol. 10, no. 30, pp. 32606–32625, Aug. 2025, doi: 10.1021/acsomega.5c02206.

[5] S. H. J. Kim, S. Park, A. A. Qutub, and C. A. Hunt, "In Silico Modeling of Blood-Brain Barrier: Agent-Based Simulation of Cerebral Glucose Transport."

[6] E. Vendel, V. Rottschäfer, and E. C. M. de Lange, "The need for mathematical modelling of spatial drug distribution within the brain," *Fluids Barriers CNS*, vol. 16, no. 1, p. 12, May 2019, doi: 10.1186/s12987-019-0133-x.

[7] S. F. Hathcock *et al.*, "Induction of P-glycoprotein overexpression in brain endothelial cells as a model to study blood-brain barrier efflux transport," *Front. Drug Deliv.*, vol. 4, July 2024, doi: 10.3389/fddev.2024.1433453.

[8] G. Sharma, A. R. Sharma, S.-S. Lee, M. Bhattacharya, J.-S. Nam, and C. Chakraborty, "Advances in nanocarriers enabled brain targeted drug delivery across blood brain barrier," *Int. J. Pharm.*, vol. 559, pp. 360–372, Mar. 2019, doi: 10.1016/j.ijpharm.2019.01.056.

[9] M. Sarafraz, M. Nakhjavani, S. Shigdar, F. C. Christo, and B. Rolfe, "Modelling of mass transport and distribution of aptamer in blood-brain barrier for tumour therapy and cancer treatment," *Eur. J. Pharm. Biopharm.*, vol. 173, pp. 121–131, Apr. 2022, doi: 10.1016/j.ejpb.2022.03.004.

[10] H. Fan, Q. Cai, and Z. Qin, "Measurement and Modeling of Transport Across the Blood–Brain Barrier," *J. Biomech. Eng.*, vol. 145, no. 8, p. 080802, Aug. 2023, doi: 10.1115/1.4062737.

[11] J. I. Morrison *et al.*, "Standardized Preclinical In Vitro Blood–Brain Barrier Mouse Assay Validates Endocytosis-Dependent Antibody Transcytosis Using Transferrin-Receptor-Mediated Pathways," *Mol. Pharm.*, vol. 20, no. 3, pp. 1564–1576, Mar. 2023, doi: 10.1021/acs.molpharmaceut.2c00768.

[12] G. James and M. Fullstone, "MODELLING THE TRANSPORT OF NANOPARTICLES ACROSS THE BLOOD-BRAIN BARRIER USING AN AGENT-BASED APPROACH."

[13] T. D. Azad, J. Pan, I. D. Connolly, A. Remington, C. M. Wilson, and G. A. Grant, "Therapeutic strategies to improve drug delivery across the blood-brain barrier," *Neurosurg. Focus*, vol. 38, no. 3, p. E9, Mar. 2015, doi: 10.3171/2014.12.FOCUS14758.

[14] E. Vendel, V. Rottschäfer, and E. C. M. de Lange, "Improving the Prediction of Local Drug Distribution Profiles in the Brain with a New 2D Mathematical Model," *Bull. Math. Biol.*, vol. 81, no. 9, pp. 3477–3507, Sept. 2019, doi: 10.1007/s11538-018-0469-4.

[15] G. R. Weatherley, R. P. Araujo, S. J. Dando, and A. L. Jenner, "Therapeutic targeting of oligodendrocytes in an agent-based model of multiple sclerosis," June 2025, doi: 10.1101/2025.06.26.661705.

[16] M. Pennisi, G. Russo, S. Motta, and F. Pappalardo, "Agent based modeling of the effects of potential treatments over the blood-brain barrier in multiple sclerosis," *J. Immunol. Methods*, vol. 427, pp. 6–12, Dec. 2015, doi: 10.1016/j.jim.2015.08.014.

[17] C. P. Spielvogel *et al.*, "Enhancing Blood–Brain Barrier Penetration Prediction by Machine Learning-Based Integration of Novel and Existing, In Silico and Experimental Molecular Parameters from a Standardized Database," *J. Chem. Inf. Model.*, vol. 65, no. 6, pp. 2773–2784, Mar. 2025, doi: 10.1021/acs.jcim.4c02212.

[18] P. A. Alves, L. C. Camargo, G. M. de Souza, M. R. Mortari, and M. Homem-de-Mello, "Computational Modeling of Pharmaceuticals with an Emphasis on Crossing the Blood–Brain Barrier," *Pharmaceuticals*, vol. 18, no. 2, p. 217, Feb. 2025, doi: 10.3390/ph18020217.

[19] E. T. C. Huang *et al.*, "Predicting blood–brain barrier permeability of molecules with a large language model and machine learning," *Sci. Rep.*, vol. 14, no. 1, p. 15844, July 2024, doi: 10.1038/s41598-024-66897-y.

[20] S. M. Chowdhury, T. Lee, and J. K. Willmann, "Ultrasound-guided drug delivery in cancer," *Sci. Adv.*, vol. 5, no. 11, Nov. 2019, doi: 10.1126/sciadv.aay1344.

Supplementary Materials

All simulation code, CT preprocessing scripts, result datasets, and high-resolution figures are available at the following OSF repository: Challenges and Strategies for Drug Delivery Across the Blood–Brain Barrier: An Engineering Perspective